LBL--33360

DE93 007663

RF Cavity Development for the PEP-II B Factory*

R. A. Rimmer

Lawrence Berkeley Laboratory
University of California
Berkeley, CA 94720

Presented at the International Workshop on B-Factories: Accelerators and Experiments, KEK, Tsukuba, Japan, Nov. 17-20, 1992.

* This work was supported by the Director, Office of Energy Research, Office of High Energy and Nuclear Physics, High Energy Physics Division, of the U.S. Department of Energy under Contract Nos. DE-AC03-76SF00098 and DE-AC03-76SF00515.

RF Cavity Development for the PEP-II *B* Factory*

R. A. Rimmer
Accelerator and Fusion Research Division
Lawrence Berkeley Laboratory, Berkeley, CA 94720, U.S.A.

ABSTRACT

This paper describes the development of an RF cavity design for the proposed PEP-II asymmetric *B* factory. The high luminosity required of PEP-II provides challenges in the design of the RF cavities, most notably in the reduced higher-order mode (HOM) impedances that must be attained and in the power that must be dissipated in the cavity walls. This paper outlines the goals set in these regards, describes how the cavity has been developed to meet them, and presents the results of measurements on a low-power test model built to verify the HOM damping scheme.

1. INTRODUCTION

Due to the high beam currents and short bunch lengths of the beams in the high- and low-energy rings of PEP-II [1], careful attention must be paid to the vacuum chamber impedances, both broad-band and narrow-band, to minimize the growth rates of beam instabilities. The single-bunch parameters are typical of present machines, placing the challenges in the domain of multi-bunch effects. In general coupled-bunch instabilities are driven almost entirely by the modes in the RF cavities. For PEP-II, the shunt impedance of the fundamental mode of the cavities has been maximized at the design frequency of 476 MHz so that the minimum number of cavities may be used. However, the HOM impedances calculated early in the design would, if undiminished, cause coupled-bunch instability growth rates far in excess of the radiation damping rate and beyond the range of a practical feedback system. It was clear from the start that some form of HOM reduction or damping would have to be developed as an integral part of the cavity design. The idea of using dedicated damping waveguides strongly coupled to the magnetic fields of the HOMs but below cut-off at the fundamental mode frequency was evaluated at LBL using a pill-box model, and the results were very encouraging [2]. At the same time numerical studies were undertaken using the MAFIA code and the Kroll-Yu method [3] which showed close agreement with the experimental results. This was sufficiently convincing that numerical simulations were used to develop the waveguide damping scheme for the PEP-II cavity and estimate the HOM reduction that could be obtained for the worst modes. A low-power test model was fabricated to confirm this performance. The current activity is directed towards a high-power model that will be tested at the full wall dissipation to verify that the design is capable of being conditioned and operated to specification.

2. CAVITY PARAMETERS

The RF system parameters required for PEP-II are shown in Table 1. Normal conducting copper cavities were chosen and the cavity shape was optimized to give the best fundamental mode performance at the design frequency of 476 MHz [4].

Table 1: RF System Parameters for PEP-II
(including the effect of the 5% gap in the beam)

PARAMETER	HER	LER
RF frequency (MHz)	476	476
Beam current (A)	1.55	2.25
Number of bunches	1658	
Number of cavities	20	10
Shunt Impedance R_S (MΩ) [a]	3.5	
Gap Voltage (MV)	0.93	0.95
Accelerating gradient (MV/m)	4.2	4.3
Wall loss/cavity (kW)	122	129
Coupling factor (β)	3.5	3.9
Unloaded Q of cavity[b]	~31000	

[a] $R_S = V^2/2P$

[b] with ports, at 40°C

Each cavity must provide a peak voltage of almost 1 MV and the shunt impedance available is estimated to be 3.5 MΩ, allowing for all coupling and damping ports and losses due to elevated wall temperature. The cavity is being designed in collaboration with AECL

*Work supported by the Director, Office of Energy Research, Office of High Energy and Nuclear Physics, High Energy Physics Division of the U.S. Department of Energy, under contract numbers DE-AC03-76SF00098 and DE-AC03-76SF00515.

TM010 mode, 0-EE-1: 489.6 MHz, R/Q=108.76 Ω, Q_0=46306, R_S=5.0 MΩ, Q_{3wg}=31926 (imperf. model).

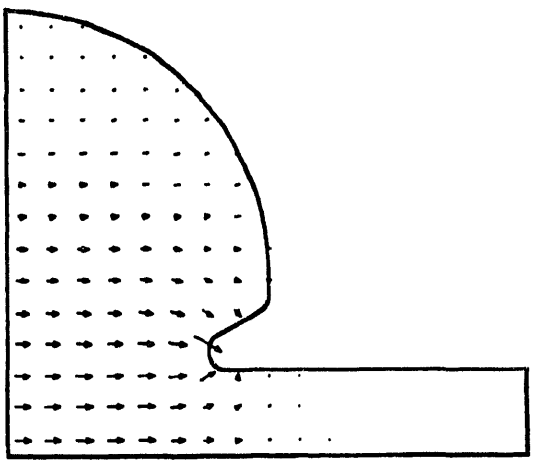

Fig.1a. Electric field of accelerating mode.

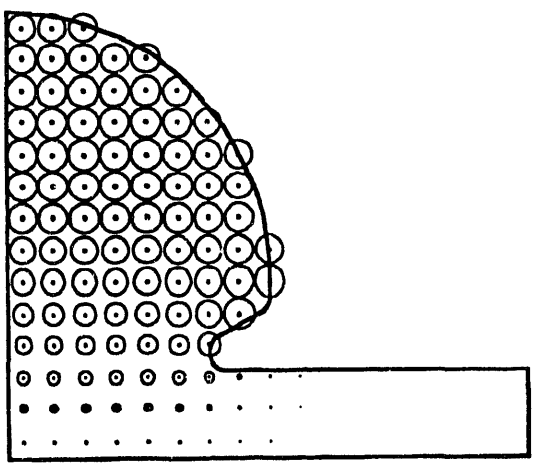

Fig.1b. Magnetic field of accelerating mode.

TM011 mode, 0-ME-1: 769.7 MHz, R/Q=44.97 Ω, Q_0=39625, R_S=1.78 MΩ, Q_{3wg}=28, R_S3wg=1.3 kΩ.

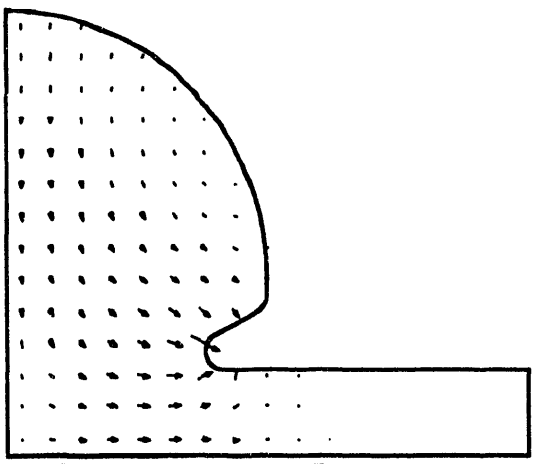

Fig.2a. Electric field of TM011 mode.

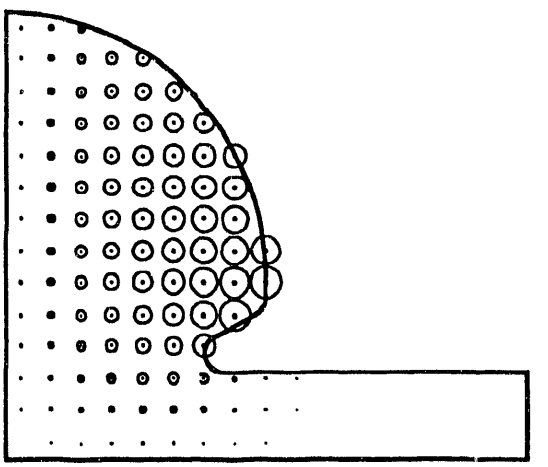

Fig.2b. Magnetic field of TM011 mode.

Chalk River Laboratory to have a cooling system that can safely handle up to 150 kW of wall power, sufficient to meet these specifications.

The 2D URMEL code [5] was used to calculate the frequencies and impedances of all the longitudinal (monopole) and transverse deflecting (dipole) modes up to the beam pipe cut-off frequency for each type of mode (1821 MHz for dipole modes, 2378 MHz for monopole modes). Figures 1 and 2 a and b show the electric and magnetic field distributions, respectively, in the cavities for the fundamental and worst higher-order longitudinal modes. Figures 3 and 4 a and b show the electric field and the azimuthal magnetic field, respectively, of the two lowest dipole modes. In the real cavity the dipole modes will be split into pairs because the symmetry of the structure is broken by the various ports.

The impedances calculated by URMEL show that the TM011 mode at about 770 MHz is by far the worst single HOM. It has a shunt impedance more than one quarter of the fundamental mode and is the mode that the damping and feedback systems must be designed to deal with. At the same time, it is important that the damping scheme does not miss any other modes because most of them could still drive the beam unstable if their Q's are high enough. Estimates of coupled-bunch instability growth rates indicate that for the TM011 mode, damping to a Q of less than or equal to 70 would allow a very practical longitudinal feedback

TE111, 1-ME-1: 679.6 MHz, R/Q@r_0=0.001 Ω, Q_0=47520, $R_S/k(r)^2$=0.001 MΩ/m, not vis. with 3wg.

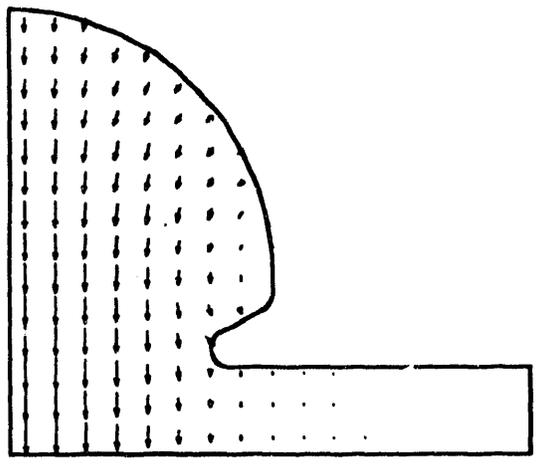

Fig.3a. Electric field of TE111 dipole mode at ϕ=0.

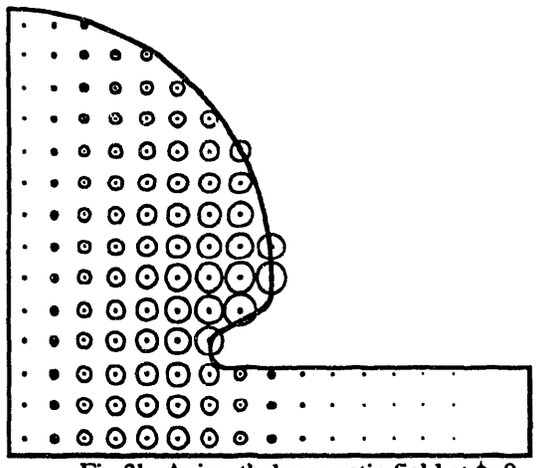

Fig.3b. Azimuthal magnetic field at ϕ=0.

TM110, 1-EE-1: 795.5 MHz, R/Q@r_0=9.88 Ω, Q_0=61076, $R_S/k(r)^2$=15.5 MΩ/m, not visible after damping.

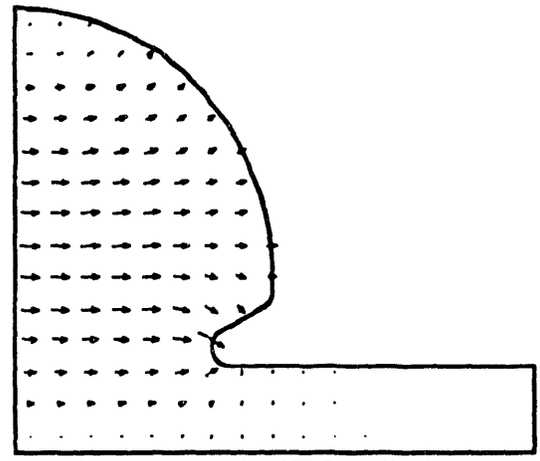

Fig.4a. Electric field of TM110 dipole mode at ϕ=0.

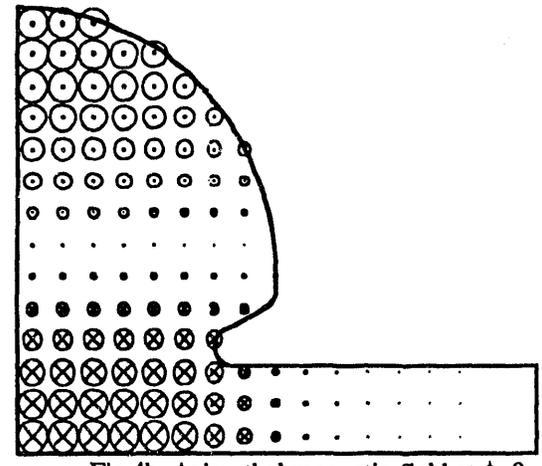

Fig.4b. Azimuthal magnetic field at ϕ=0.

system. This Q value corresponds to a residual impedance of about 3.2 kΩ at 770 MHz.

Other modes with lower initial impedances may not need to be damped as much but their residual impedances should be less than this value, reduced by the frequency dependence f/frf (less driving impedance can be tolerated at higher frequency). The estimated allowed values for each mode are shown in Table 2a, column 10. The feedback system is designed to handle these driving impedances and an initial coupled-bunch phase disturbance of 30 mrad (or larger single-bunch errors caused during injection).

For transverse beam motion, the feedback system must be sized to handle the growth rates of modes driven by the resistive-wall impedance and the target is to damp deflecting cavity modes to an extent where the growth rates they produce are handled by the same system. The target value for the transverse impedance of the dipole modes is 117 kΩ/m.

3. WAVEGUIDE DAMPING SCHEME

The damping scheme has to reduce the impedances at the HOM frequencies by coupling energy out of the cavity to external loads. At the same time it is desirable to have the minimum adverse effect on the fundamental-mode performance. A waveguide damping scheme satisfies these conflicting objectives by operating as a high-pass filter, propagating away energy at the HOM frequencies, above the waveguide cut-off,

while strongly rejecting the fundamental mode below cut-off, leaving it trapped in the cavity. There is an inevitable loss of some fundamental-mode performance because part of the cavity wall is removed and the effective shape of the cavity is changed, but by keeping the apertures small and using the best position in the wall to couple to the target HOMs the degradation can be minimized. There is, of course, a trade-off between the strength of coupling to the HOMs and the loss in fundamental-mode impedance.

For the PEP-II cavity, the waveguides have a cut-off frequency of 600 MHz which allows all HOMs to propagate while being far enough above the 476 MHz fundamental to give good rejection. The waveguides open into the cavity through slightly smaller irises to preserve the cavity fundamental mode as much as possible, while providing sufficient coupling to reduce the worst HOMs to safely below the target impedances. It is planned that the HOM power will be dissipated in loads at the ends of these waveguides, inside the vacuum envelope. It is thought that this is preferable to trying to build very broad-band windows to external loads.

Looking at the azimuthal magnetic field Hϕ at the cavity wall for the HOMs in Figs. 1b and 2b and for the rest of the modes it is clear that for most of them there are places where the field goes zero. For modes that are anti-symmetric in Hϕ about the cavity center (URMEL calls these x-ME-x modes, M being for the "magnetic" boundary condition in the center of the cavity), the azimuthal magnetic field goes to zero at the center of the cavity. Hence none of these modes will couple strongly to the fundamental mode coupler. Since the HOM damping waveguides are designed to couple to the azimuthal magnetic field they must be placed on the cavity wall such as to avoid any of the points where the HOM fields go to zero, or that HOM will remain undamped.

The TM011 mode has only one zero in the Hϕ field, in the center of the cavity, so a damping waveguide placed anywhere else on the perimeter will couple to the mode and provide some damping. The field strength is maximum close to the base of the nose-cone, see Fig. 2b, but there is not enough wall circumference at this point to put the waveguides. The optimum position is somewhere in between but many other HOMs have zero field points in this region and the locations of these zeros are shown in Fig.5. Note that even those symmetric (EE) dipole modes that appear to have Hϕ field in the center of the cavity will have a degenerate twin that may be oriented to escape damping. Figure 5 also shows the magnetic field distribution of the TM011 mode. Note that all HOMs have some magnetic field at a point 30° up on the curved part of the wall, and that the TM011 mode has strong field there. This is therefore a good place for the damping waveguides. Figure 6 shows a 1" high waveguide at this location. Three damping waveguides are used which preserve symmetry in the fundamental mode and catch all HOMs up to those with sextupole variation around the azimuth.

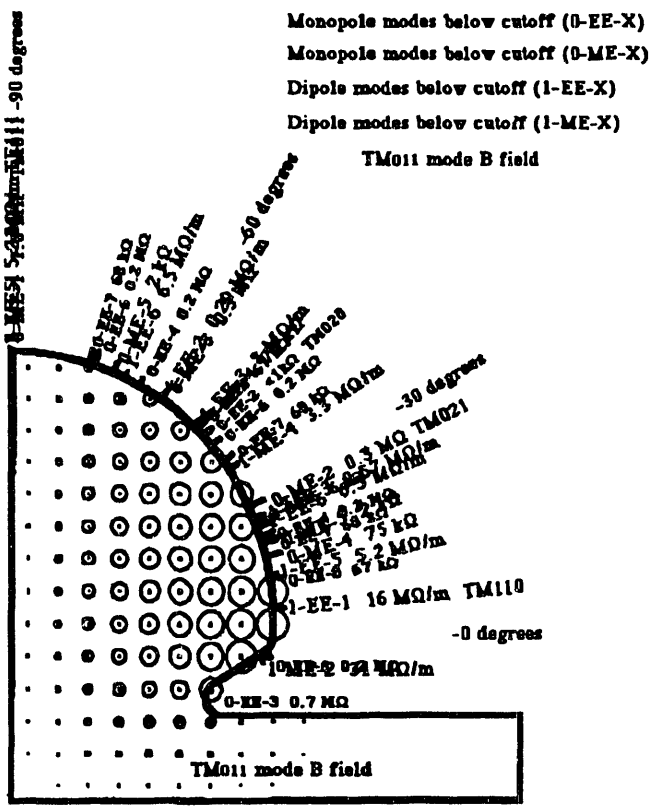

Fig.5. HOM zero-field points + TM011 magnetic field.

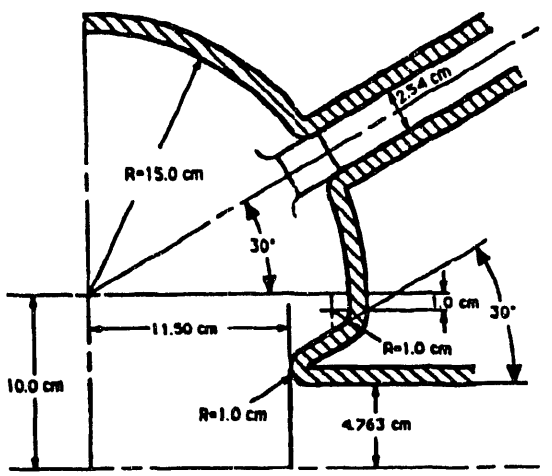

Fig.6. Location of damping waveguide in LPTC.

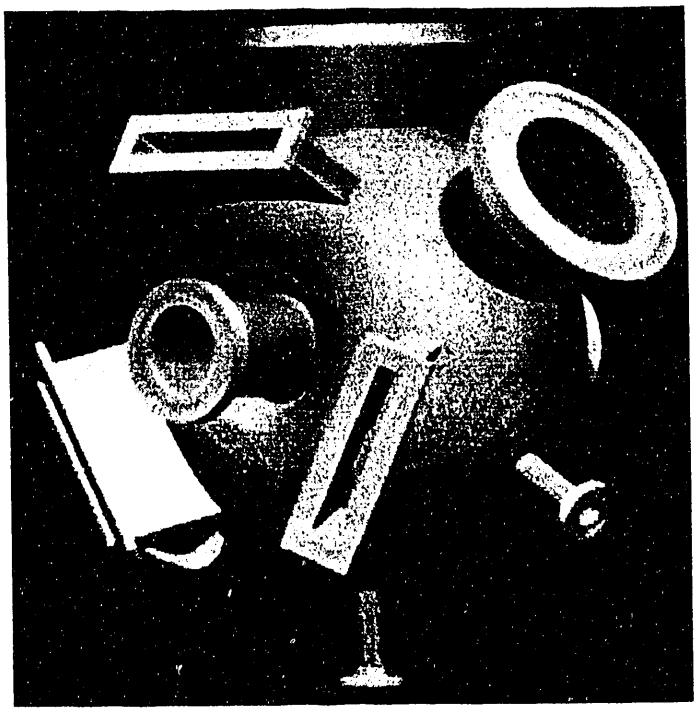

Fig.7. CAD drawing of low-power test cavity.

Computer simulations of this geometry indicated that sufficient damping would be obtained for the worst HOMs, and this was the shape used for the Low-Power Test Cavity (LPTC). The CAD drawing of the proposed design is shown in Fig.7 and the cavity as delivered is pictured in Fig.8. The low-power model was fabricated by electro-forming onto an aluminum mandril with the ports made separately in copper and brass and "grown" on during the process. The aluminum mandril was then etched out to leave the finished cavity. This resulted in a quite good inside surface, although not as good as would be required for a high-power model. Hence the maximum Q obtained in the lab tests, though acceptable, was not expected to be representative of a real production cavity. However the Q's of the HOMs should be determined by the coupling to the external loads, so the model is a valid test of the damping method.

4. MEASUREMENTS OF HOMS IN THE LPTC

The low-power test cavity was mounted in a fixture in the RF test lab at LBL with beam-pipe extensions bolted on and all of the other ports blanked off with plugs made to conform to the cavity inner wall profile and making contact with the cavity body through spring fingers. Small electric field antennas were introduced though the beam pipes to excite the cavity and the transmission response between these probes (S21) was measured using an HP 8510C network analyzer. In this configuration, with no damping, the modes were visible as discrete resonances and their frequencies were very close to the URMEL calculations, allowing all of the important modes below cut-off to be identified. Tables 2a and 2b list the modes and their calculated and measured properties. Figures 9a-13a show the undamped response of the cavity up to and slightly above the monopole mode beam-pipe cut-off, in five frequency ranges. The peaks corresponding to the monopole and dipole modes are labelled and their unloaded impedances are listed for reference. Note that the relative amplitudes of the peaks do not give a good indication of their relative impedances because the network analyzer sweep of 801 data points may not accurately resolve the sharpest peaks in these wide spans and the antennas couple differently to the different modes due to their positions in the cavity and their own frequency response. For determination of the Q's of the individual modes in subsequent measurements much narrower frequency sweeps were used to properly resolve the peaks. Note also that above the TM01 cut-off of the beam pipe, Fig.13a, the character of the response is quite different. At these frequencies both monopole and dipole modes can escape into the beam pipes and the sharp structure of the discrete modes below cut-off gives way to a much more "smeared out" behavior. Resonant modes are not generally thought to cause problems at frequencies above cut-off, although energy can be lost by the beam through wake-field effects.

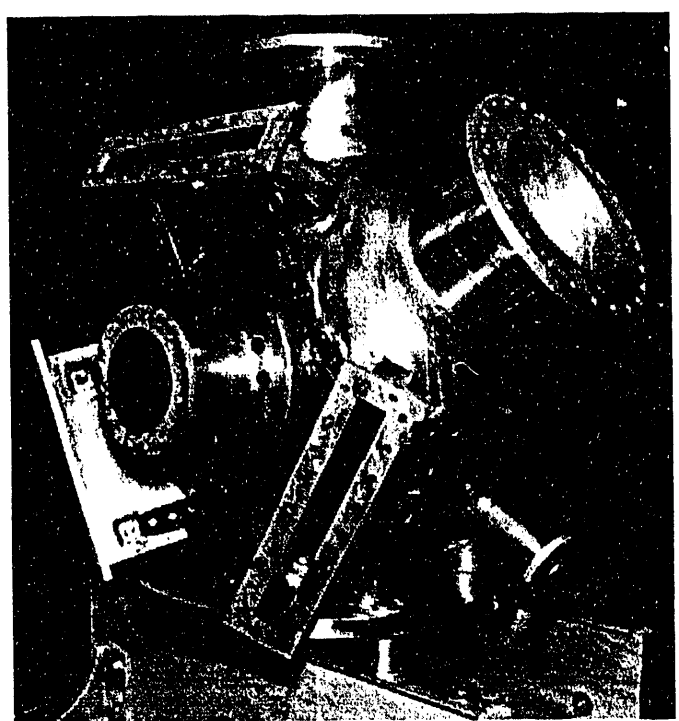

Fig.8. Completed LPTC awaiting waveguides.

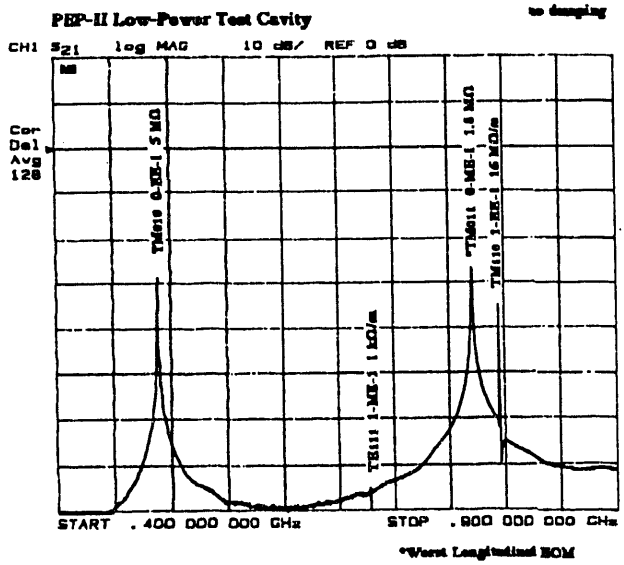

Fig.9a. Fundamental mode and first three higher order modes in the LPTC without damping. Note the strong response from the TM011 mode which is the worst longitudinal HOM.

Figure 9b shows the effect of adding one HOM damping waveguide to the cavity while leaving the others sealed. Apart from a small frequency shift, the fundamental mode is not significantly changed but the first and worst monopole HOM, TM011, is loaded to a Q of less than 35 and a frequency of about 760 MHz. This Q is already half of the target value of 70 from the

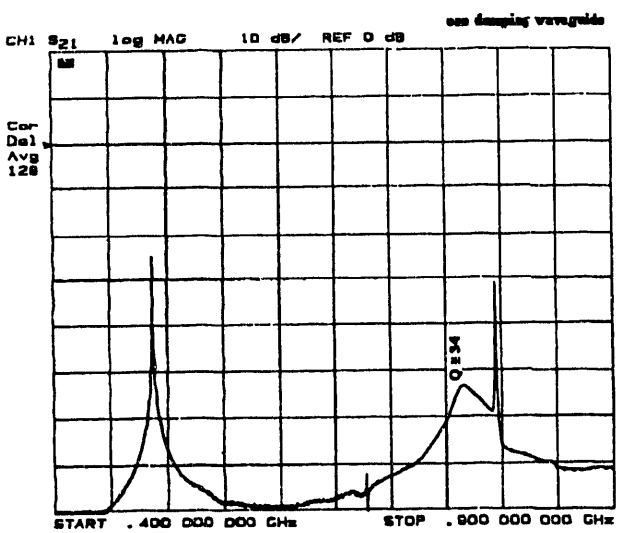

Fig.9b. Fundamental mode and first three HOMs in the LPTC with one damping waveguide. The TM011 mode and one orientation of the TM110 dipole mode are strongly damped.

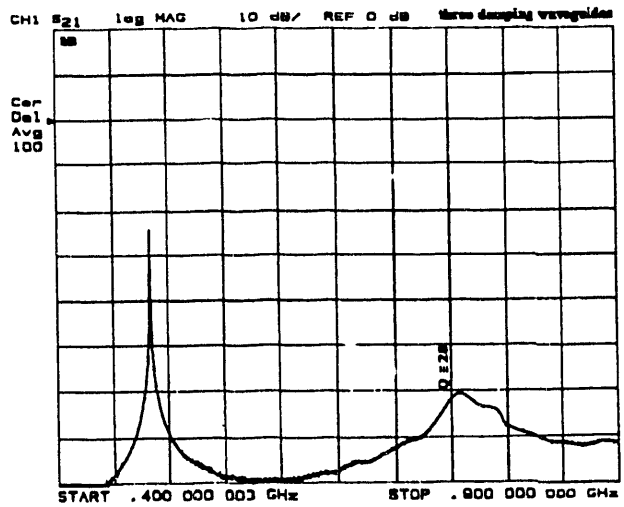

Fig.9c. Fundamental mode and first HOMs in the LPTC with three damping waveguides. The TM011 mode is further damped and both orientations of the dipole mode are strongly suppressed.

feedback system specification. One orientation of the TM110 dipole mode at 795 MHz is heavily damped but the other orientation is still clearly visible. Similar results are seen in the other frequency ranges.

Figures 9c and 10b-13b show the response with all three waveguides attached and terminated, like the first one, in loads made of epoxy-ferrite mixture. These

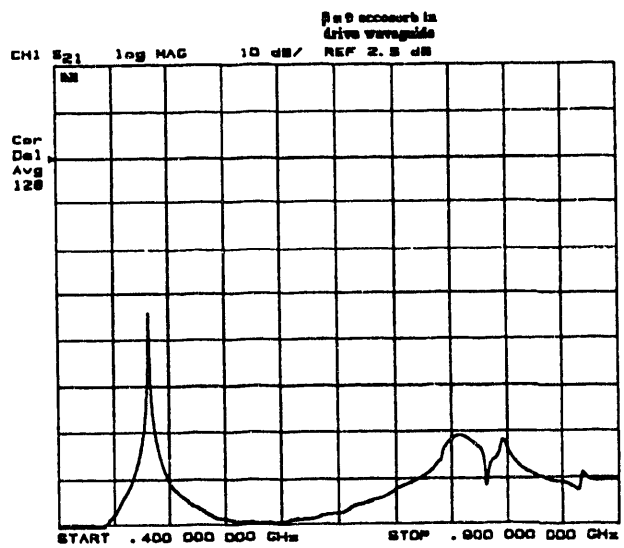

Fig.9d. Fundamental mode and first HOMs with three damping waveguides and PEP loop fundamental-mode coupler. Note that some new structure appears in the spectrum because of the loop.

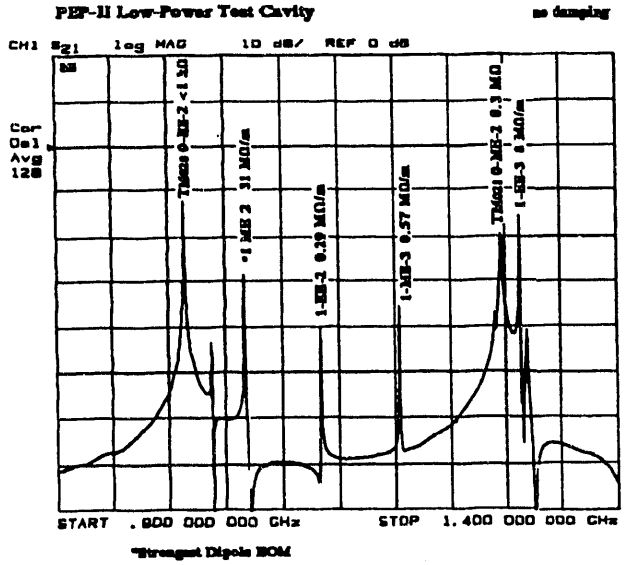

Fig. 10a. Undamped HOMs between 900 and 1400 MHz in the LPTC. The 1-ME-2 mode at 1064 MHz is the worst deflecting (dipole) mode.

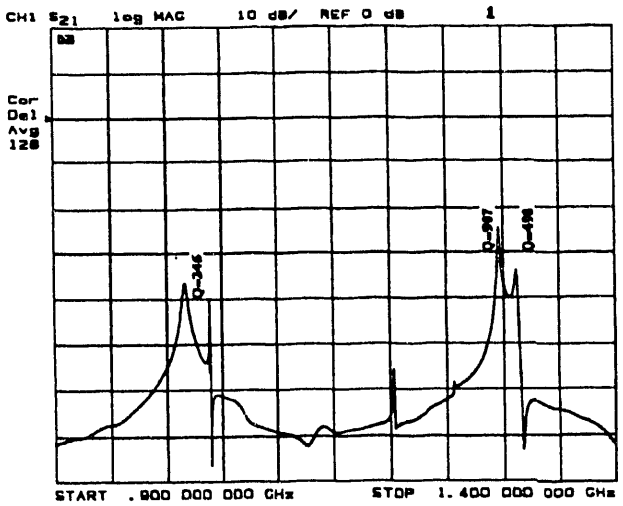

Fig. 10b. HOMs between 900 and 1400 MHz in the LPTC with three damping waveguides. Most of the modes are strongly damped.

loads are at the edges of the waveguides and have long tapers to simulate the high-power loads that would be used in the real cavities and provide low reflection over a wide frequency range. With all three waveguides open, the TM011 mode is further reduced to a Q of approximately 28 (the Q is uncertain because the response is no longer an ideal resonant curve as the tails of the modes overlap). This represents a reduction of more than three orders of magnitude from the calculated unloaded Q_0 of >39600. Both orientations of the TM110 dipole mode are strongly damped and are barely visible at the edge of the TM011 response.

In Fig. 10b, the TM020 monopole mode is still visible at 1016 MHz, but its Q is less than 250 and its residual impedance is very small, one thousandth of the target value at that frequency. The 1-ME-2 mode, the worst dipole HOM, 1-EE-2 1-ME-3 and 1-EE-3 dipole modes are all damped to safe levels, the latter being visible at 1311 MHz with a Q of about 500.

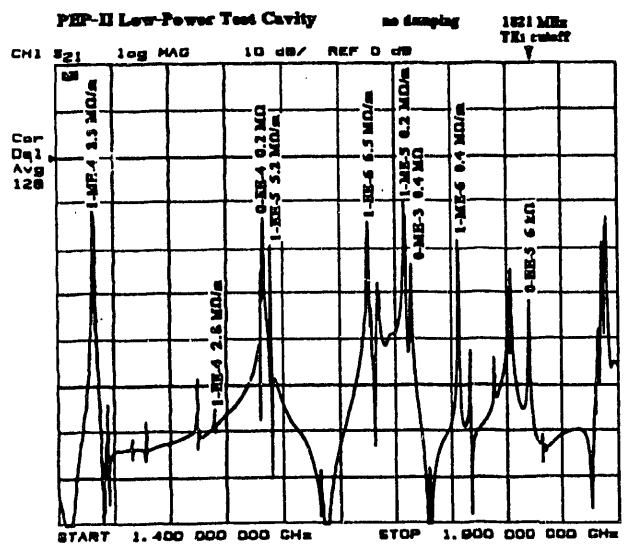

Fig. 11a. HOMs between 1.4 and 1.9 GHz, monopole and dipole modes only labeled. Note cut-off frequency of the TE11 mode in the beam pipe at 1.821 GHz.

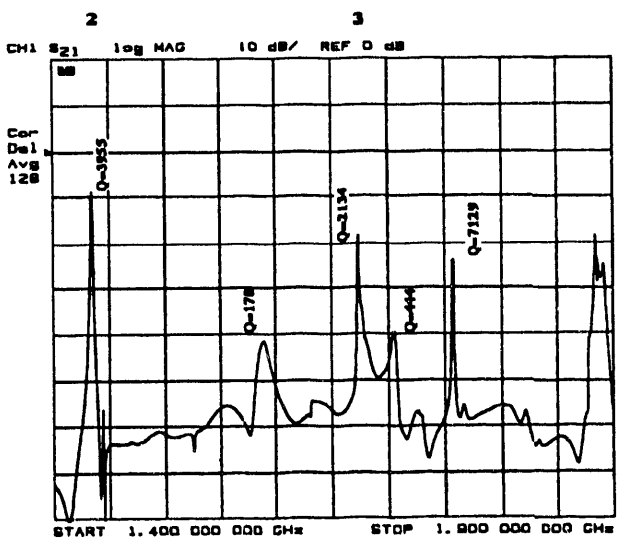

Fig. 11b. HOMs between 1.4 and 1.9 GHz with three damping waveguides. Note that many modes are no longer visible and most others are strongly damped.

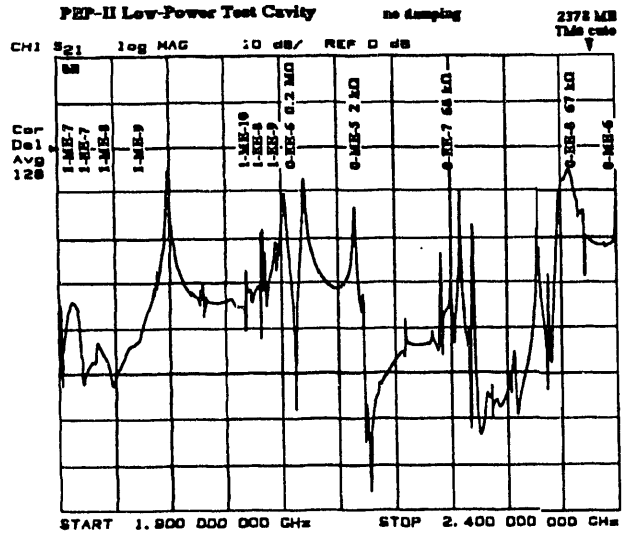

Fig. 12a. HOMs between 1.9 and 2.4 GHz with no damping. Note TM01 waveguide mode cut-off in the beam-pipe at 2378 MHz.

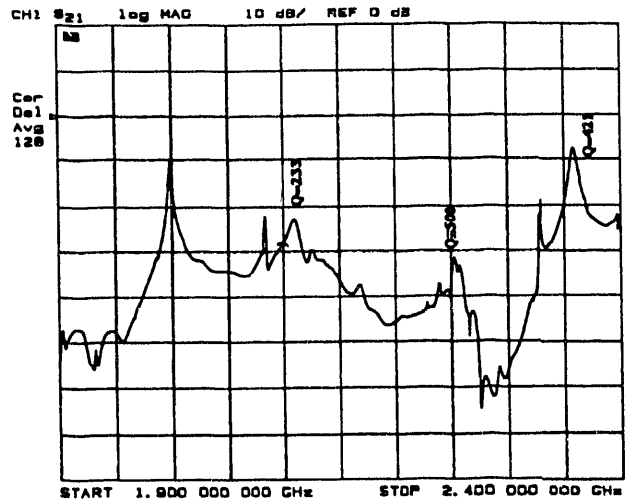

Fig. 12b. HOMs between 1.9 and 2.4 GHz with three damping waveguides. No modes have residual impedance greater than the target values.

The TM021-like 0-ME-2 monopole mode is still visible at 1296 MHz and although its Q is reduced to about 907 its initial impedance is high and its residual impedance is about three times the target value. However, there is considerable safety margin in the feedback specification, as is described later in the section on feedback simulations and, furthermore, more damping may be possible through the drive port and pumping structure.

Figure 11b shows many fewer modes visible after damping than in fig. 11a and, of these, only the 1-ME-4, 1-EE-6, 0-EE-4 and 1-ME-6 modes have significant residual impedance. The last two of these are sufficiently damped but the first two exceed the target value for the transverse feedback system by factors of about 3. As with the longitudinal case the safety margin in the feedback system and additional damping from other ports are expected to eliminate problems from these too. Figures 12b and 13b show good damping with no more HOMs left with troublesome impedances.

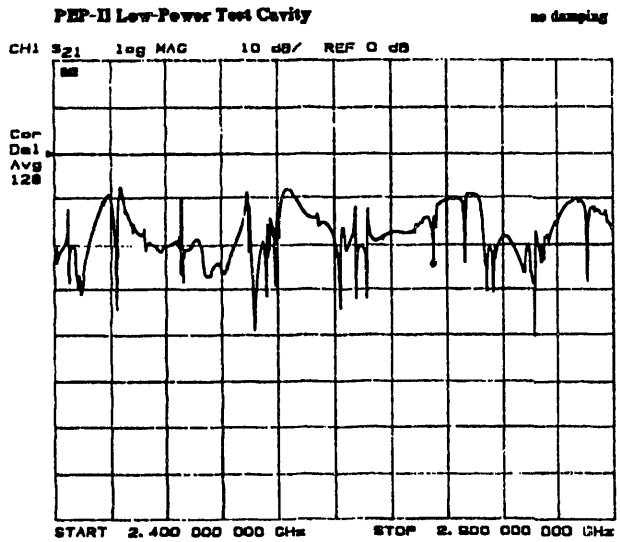

Fig. 13a. HOMs between 2.4 and 2.9 GHz with no waveguides. Both monopole and dipole modes can couple to the beam pipes.

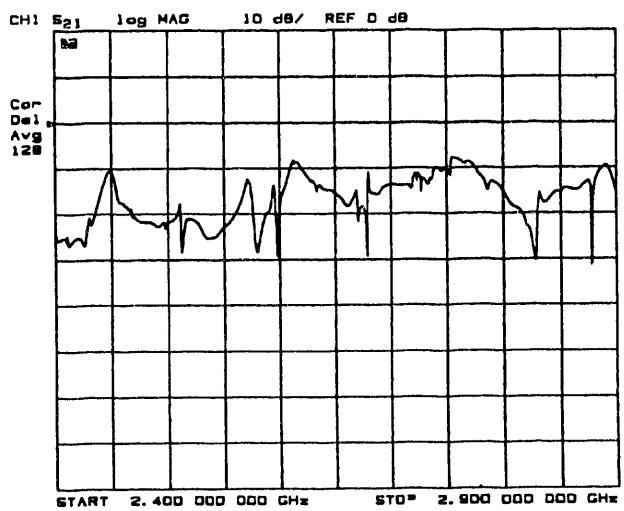

Fig. 13b. HOMs between 2.4 and 2.9 GHz with three waveguides. Even above cut-off the spectrum is cleaner with the damping waveguides than without.

Table 2a. Properties of the longitudinal (monopole) modes below the beam-pipe cut-off calculated by URMEL and measured in the low-power test cavity. The last three columns show the effective impedance estimated by using the calculated R/Q and the measured Q_L, (R/Q x Q_L, kΩ), the target impedance per cavity from the longitudinal feedback system and the fraction used by the modes.

*note that the model as constructed is not a good test of the fundamental mode Q.

	MODE TYPE	FREQ (MHz)	R/Q (Ω)	URMEL Q's	Rs (MΩ)	Meas F (MHz)	MEAS Q's	R/Q x Q_L (kΩ)	target (kΩ)	fract. of target
TM010	0-EE-1	489.57	108.76	46306	5.036	484	*31926	3472.277	5.0	694
TM011	0-ME-1	769.78	44.97	39625	1.782	758	28	1.259	3.2	0.394
TM020	0-EE-2	1015.38	0.01	41383	0.000	1016	246	0.001	2.4	0.001
	0-EE-3	1291.02	7.68	90188	0.692	not visible after damping			1.9	
TM021	0-ME-2	1295.61	6.57	40326	0.265	1296	907	5.955	1.9	3.185
	0-EE-4	1585.46	5.06	42724	0.216	1588	178	0.901	1.5	0.591
	0-ME-3	1711.62	4.75	85135	0.404	not visible after damping			1.4	
	0-EE-5	1821.89	0.06	107874	0.006	1821	295	0.018	1.3	0.013
	0-ME-4	1890.98	1.68	44492	0.075	not visible after damping			1.2	
	0-EE-6	2103.39	3.52	66780	0.235	2109	233	0.820	1.1	0.713
	0-ME-5	2161.89	0.02	84386	0.002	2168	201	0.004	1.1	0.004
	0-EE-7	2252.16	1.21	55944	0.068	2253	500	0.607	1.1	0.564

Table 2b, Properties of the deflecting (dipole) modes below the beam-pipe cut-off calculated by URMEL and measured in the low-power test cavity. The last three columns show the effective transverse impedance estimated by using the calculated R/Q at the beam-pipe radius and the measured Q, (R/Q/k(r)^2 x Q_L, kΩ/m), the target impedance from the transverse feedback system (resistive-wall impedance) and the fraction used by the modes.

	MODE TYPE	FREQ (MHz)	R/Q (Ω@ro)	R/Q/(kr)^2 (Ω@ro)	URMEL Q's	R/k(r)^2 (MΩ/m)	Meas F (MHz)	MEAS Q's	R/Qk(r)^2*Q (kΩ/m)	target (kΩ/m)	fract. of res. wall
TE111	1-ME-1	679.57	0.001	0.002	47520	0.001	not visible after damping				
TM110	1-EE-1	795.46	9.876	15.263	61076	15.531	not visible after damping				
	1-ME-2	1064.81	31.990	27.590	50048	30.794	not visible after damping				
	1-EE-2	1133.16	0.320	0.243	49771	0.287	1141	112	0.650	117	0.006
	1-ME-3	1208.21	0.385	0.258	87745	0.573	1203	1588	10.323	117	0.088
	1-EE-3	1313.21	10.336	5.861	50189	8.090	1311	498	80.142	117	0.685
	1-ME-4	1429.01	5.999	2.873	38150	3.280	1435	3955	341.502	117	2.919
	1-EE-4	1541.02	2.065	0.850	102408	2.809	1554	59	1.624	117	0.014
	1-EE-5	1586.23	5.262	2.045	76118	5.171	1588	178	12.107	117	0.103
	1-EE-6	1674.16	14.732	5.140	36130	6.512	1674	2134	384.567	117	3.287
	1-ME-5	1704.41	0.285	0.096	52856	0.181	1704	444	1.521	117	0.013
	1-ME-6	1761.93	0.330	0.104	92516	0.355	1757	7129	27.283	117	0.233

5. FEEDBACK SYSTEM SIMULATIONS

Simulation programs have been used to study the parameters of the proposed coupled-bunch feedback systems and can also be used to predict the behavior of the beam subject to the driving impedances measured in the test cavity. The longitudinal feedback system is being designed to handle a coherent coupled-bunch mode amplitude of 30 mrad but can tolerate much larger offset of a single bunch, for example during injection.

Simulations of the longitudinal feedback system show that even using the residual impedances measured in the test cavity, a few of which are slightly higher than the target values, the beam is still stable and transients are quickly damped. Figure 14 shows a simulation in which the beam stays stable to within 2 mrad

longitudinal phase variation (the quantization level in the phase detector) and on turn 2000 one bunch is given a kick of 30 mrad. The bunch remains stable and it is quickly damped back to its original small amplitude. A transverse feedback simulation program is presently being developed and is expected to show similar behavior using the measured transverse impedances.

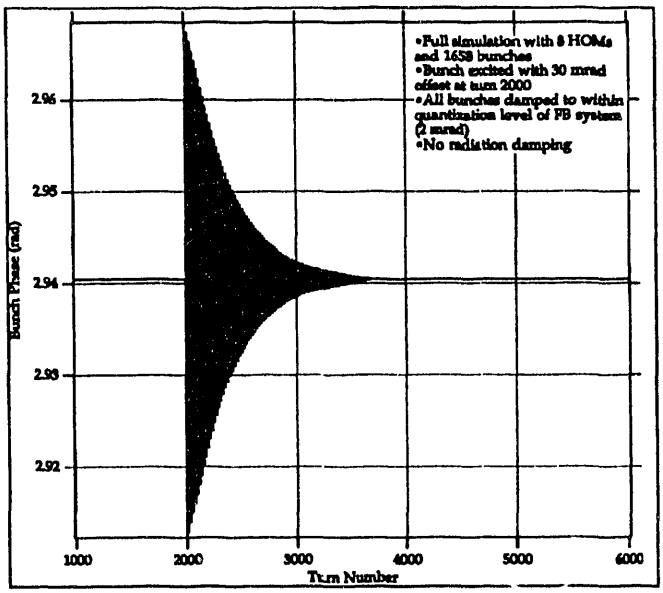

Fig.14, Simulation of longitudinal bunch motion with feedback on and measured HOM impedances.

6. DRIVE COUPLER

Addition of a drive coupler to the cavity will perturb the fields of many of the HOM. To test this a loop coupler from one of the original PEP cavities was introduced into the low-power cavity to see how this affects the damping. As seen in fig. 9d and described above this has the effect of tuning some of the HOMs but does not appear to cause any of the harmful modes to become less well damped. In fact, the additional damping from the drive port is *helpful* to the three worst remaining HOMs. Aperture coupling schemes are also being studied for use in the final cavities and the high-power test cavity will include such a port.

7. HIGH-POWER TEST CAVITY

The next important R&D step is to build a high-power test cavity (HPTC) to prove that this kind of low-HOM design can be conditioned and operated at the 150 kW wall dissipation required for PEP-II. To speed up the design and fabrication of the high-power cavity it is planned to use a PEP loop coupler for the drive. These have been tested in the PEP cavities to 200 kW and should be more than adequate for the task. The final cavity will have to take almost 500 kW with full beam current and an improved coupler design will be required.

The HPTC is being designed in collaboration with AECL Chalk River Laboratories. This work includes detailed cooling and thermal stress simulations and the development of a possible fabrication plan. The highest power density in the cavity is at the corners of the damping waveguides. Removing the heat from these locations and reducing the thermal stresses to acceptable levels have been the main challenges in the design of the HPTC. This work is well advanced and it is hoped that the high-power cavity will be ready for testing at SLAC in about one year.

8. CONCLUSIONS

The basic shape of PEP-II *B* factory RF cavity has been chosen for maximum fundamental mode shunt impedance and every effort has been made to preserve this performance in subsequent steps. A waveguide damping scheme has been developed through computer simulations and test models that shows great promise for substantially reducing the impedances of higher-order modes. A design for the PEP-II cavity has been developed using three damping waveguides. A full-size low-power model has been built and tested and confirms our expectations. The impedance of the worst HOM in the cavity, the TM011 longitudinal mode, has been be reduced by more than three orders of magnitude. Plans for a high-power test cavity are well advanced and it is hoped that this will be ready for testing in about a year.

6. ACKNOWLEDGEMENTS

This paper presents the work of numerous people besides the author, from the three collaborating laboratories, SLAC, LBL and LLNL and beyond.

REFERENCES

[1] "An Asymmetric B-Factory based on PEP," Conceptual Design Report, LBL PUB-5303, SLAC 372

[2] N. Kroll, D. Yu, "Computer Determination of the External Q and Resonant Frequency of Waveguide Loaded Cavities," SLAC-PUB-5171.

[3] F. Voelker, G. Lambertson, R. Rimmer, "Higher Order Mode Damping in a Pill Box Cavity," Proc. PAC, San Francisco, May 6-9th, 1991, pp 687-689 LBL-30625.

[4] R. Rimmer et. al., "An RF Cavity for the B-Factory", Proc. PAC, San Francisco, May 6th-9th, 1991, pp819-21.

[5] "Reports at the 1986 Stanford Linac Conference., Stanford, USA, June 2-6 1986," DESY M-86-07, June 86

END

DATE
FILMED
4/8/93